Single-Walled Carbon and Boron Nitride Nanotubes as Tyrphostin AG 528 Cancer Inhibitor Carriers

Eshraq Ahmed Abdullah[1, *]

[1]Department of Chemistry, Faculty of Education, Taiz University, Taiz, 009674, Yemen

Email address:
ali123456yemen@gmail.com (Eshraq Ahmed Abdullah)

[*]Corresponding author
Eshraq Ahmed Abdullah, Department of Chemistry, Faculty of Education, Taiz University, Taiz, 009674, Yemen
Tel no: +(967) (4). (257802)
Mobil no: +(967) (770120594)
https://orcid.org/0000-0001-9698-6203

To cite this article:

Abstract:
Chemotherapeutic drug delivery systems that are based on nanotechnology have received considerable attention in cancer treatment due to their ability to enhance the bioavailability of drugs and protect them from enzymatic degradation. Each drug delivery carrier has its own advantages. Therefore, the way to select the most suitable delivery carrier remains a key challenge. Recently, computational approaches have been utilized to explain molecular interactions of the anticancer drug when they are brought into contact with the nanocarrier drug delivery. Thus, this study aims at identifying the molecular interaction forces of a Tyrphostin cancer inhibitor when it comes into contact with single-walled carbon nanotubes and boron nitride nanotubes drug delivery carriers. The effect of the nonbonding interactions on their electronic and optical properties was investigated using Density Functional Theory and Monte Carlo simulation. The Tyrphostin cancer inhibitor was successfully attached to the nanotube surface by weak van der Waals forces of -CH-π and π-π stackings. A highly-repulsive behavior in a hydrophobic region makes the carriers effective promising drug delivery candidates for insoluble anticancer drugs. Both Tyrphostin/carrier complexes have similar structures; however, the binding energy indicates that the Tyrphostin inhibitor was preferentially adsorbed onto the single-walled carbon nanotubes and the optimized geometry is more stable. The molecular interaction produces a significant bathochromic shift on the optical spectrum of the Tyrphostin inhibitor and reduces the molecular band gap of the boron nitride carrier. While the Tyrphostin/single-walled carbon nanotube can act as a better visible-light response drug delivery system, the boron nitride nanotube becomes more sensitive to detect the Tyrphostin inhibitor on its surface.

Keywords: Drug delivery, Tyrphostin, DMol3 module, Boron nitride nanotube, Single walled carbon nanotube.

List of Abbreviations

ATP	Adenosine Triphosphate	HBD	Hydrogen Bonding Donor
BNNT	Boron Nitride Nanotube	HCTH	The Hamprecht-Cohen-Tozer-Handy Functional

COSMO	Conductor-like Screening Model	HER2	Human Epidermal Growth Factor Receptor 2
DFT	Density Functional Theory	HOMO	The Highest Occupied Molecular Orbital
DND	Double-Numerical Basis Set	LUMO	The Lowest Unoccupied Molecular Orbital
DOS	Density of States	MC	Monte Carlo Simulation
EPS	Electrostatic Potential Surface	MEP	Molecular Electrostatic Potential
GGA	Generalized Gradient Approximation	SWCNT	Single-Walled Carbon Nanotube
HBA	Hydrogen Bond Acceptor	TD-DFT	Time-Dependent-Density Functional Theory

1. Introduction

In pathologies such as cancer signaling proteins, which are used to link internal and external stimuli to changes in cell morphology and gene expression, are disrupted by gene mutations. Consequently, chromosomal translocations lead to abnormal growth and blocked differentiation. Returning signaling proteins to their inactive state is a way to reduce inflammation and cell apoptosis [1]. Over the past few decades, low-molecular-weight compounds, Tyrphostins, have been selected as potent inhibitors of protein tyrosine kinases [2]. In this respect, Tyrphostin AG 528 is suggested as an inhibitor of human epidermal growth factor receptor 2 (HER2) signaling, which plays an important role in the development of breast cancer [3]. Kinetically, the inhibition mechanism of Tyrphostin is due to its ability to compete with Adenosine triphosphate (ATP) for the ATP binding sites [4].

To develop the therapeutic efficiency of Tyrphostin, drug delivery carriers transport the inhibitor to a specific location within the body [5]. With modern technology, Nanoparticles and nanotubes are designed to deliver drug molecules into target regions [6]. Among them, the single-walled carbon nanotube (SWCNT) is the most famous drug carrier used to attack carcinogenic cells due to its high chemical stability [7]. The small diameter of SWCNT develops the insertion and the slow release of the drug [8]. However, the low cytotoxicity of SWCNT may restrict its use in biomedical applications. Therefore, boron nitride nanotube carrier (BNNT) has been introduced as an alternative carrier due to its structural stability, high partial charges, and water permeation coefficients [9]. Since the BNNT is composed of B and N atoms, its electronic structure and chemical and physical properties are expected to be rather different from that of SWCNT. Moreover, the charge distribution is asymmetric due to the electronegative difference in B–N bonds as compared to the C–C bonds [10].

Over the years, computational and experimental studies have focused their efforts on elucidating the interaction mechanism of the drug with nanomaterial carriers. In this connection, Sheikhi et al. (2019) calculations showed that intermolecular hydrogen bonds were the main interaction forces that stabilize the loading process of the Tyrphostin molecule onto the carbon nanotube (6,6-6) surface [8]. However, according to Mortazavifar *et al.* (2019) study, the intermolecular hydrogen bonds have been used as the interaction forces to stabilize the Hydroxyurea drug inside the boron nitride and carbon nanotubes as their surfaces functionalized hydroxyl groups. Otherwise, the stabilization mechanism was ascribed to the weak van der Waals forces [11].

Fan et al. (2017) explained that the weak van der Waals forces used to stabilize the amino acid molecules on the boron nitride surface were the $\pi - \pi$ and $-CH - \pi$ stacking interactions [12].

The present study aims to describe the electronic and optical properties of Tyrphostin/SWCNT and Tyrphostin/BNNT complexes in comparison with their isolated systems in order to draw a simple picture of nonbonded interactions. To achieve the objective of the study, the SWCNT with the stoichiometry of $C_{96}H_{24}$, BNNT with the stoichiometry of $H_{24}B_{48}N_{48}$, and the Tyrphostin inhibitor with the stoichiometry of $C_{18}H_{14}N_2O_3$ have been selected as carriers and as a drug model, respectively. First, these title compounds were relaxed on the DMol3 module using a generalized gradient approximation. After that, a Monte Carlo (MC) simulation was carried out to determine the adsorption minimum energy. Finally, the molecular orbital contributions, the optical properties, the density of states, the effect of solvent properties, and the electrostatic potential of the cancer inhibitor, carriers, and the considered complexes have been analyzed using *ab initio* density functional theory (DFT) to have a better understanding of the interaction nature. To the best of our knowledge, no available literature had ever made a comparative study of SWCNT and BNNT as potential Tyrphostin drug delivery carriers.

2. Computational Methods

The nonbonded interaction between SWCNT and BNNT in which the ends of the tube were saturated with hydrogen atoms to reduce the boundary effects in the solvent water was theoretically simulated. First, adsorbate, carrier, and their complexes were relaxed using a DMol3 module executed in the BIOVIA Material studio 2017 software at a generalized gradient approximation (GGA) [15]. Then, the Monte Carlo search implemented in an adsorption locator module was performed to screen the most stable configuration of Tyrphostin adsorbate on the SWCNT and BNNT carriers, respectively. Finally, quantum mechanics was used to elucidating the impact of the adsorption process on the structural features of the optimized complexes [17, 18]. At a greater length, an orbital overlapping (Density of states), molecular orbital (HOMO – LUMO) properties, and electrostatic potential surface are acquired using the exchange and correlation functional of Hamprecht-Cohen-Tozer-Handy (HCTH/407) with DND basis set and an all-electron approach at the GGA level of theory. To examine the influence of the solvent on the adsorption behavior, single-point energy calculations were carried out to generate the sigma profiles of isolated components and their complexes using the Conductor-like Screening Model (COSMO) with a dielectric constant of 78.

3. Results and Discussion

3.1. Adsorption Locator Studies

To identify the energetically stable adsorption sites, the Monte Carlo search was carried out using an adsorption locator module. The most stable geometries of the Tyrphostin/SWCNT and the Tyrphostin/BNNT complexes within the minimum intermolecular distances between the most active adsorption sites are shown in Figure 1. The close contact calculation shows that the absolute distance occurs in the range of more than 3Å. This interaction range means that the Tyrphostin and carriers have a physical adsorption-like bonding. The reason for this behavior may be attributed to a hydrophobic character of the SWCNT and BNNT nanocarriers arising from typical sp^2 hybridized orbitals [13]. These delocalized electrons develop a repulsive effect with the electron-rich nitrogen and oxygen atoms. The adsorption energy of stable sites is outlined in Table 1. The adsorption energy value for the most stable configuration was estimated to

be -4.58x10^4 kcal/mol for both Tyrphostin /nanocarrier complexes. This indicates the similarity of interaction forces involved in the adsorption. The negative value of the adsorption energy suggests that the interaction between Tyrphostin and a nanocarrier surface is spontaneous and thermodynamically favorable [14].

Table 1. The adsorption energy values for the most stable configurations

Energy (E) kcal/mol	E_{Total}	$E_{\text{Adsorption}}$	$E_{\text{Rigid adsorption}}$	$E_{\text{Deformation}}$	dE_{ad}/dNi
Tyrphostin/SWCNT	41.58	-4.58x10^4	-26.50	-4.579x10^4	-4.58x10^4
Tyrphostin /BBNT	40.60	-4.58x10^4	-28.08	-4.579x10^4	-4.58x10^4

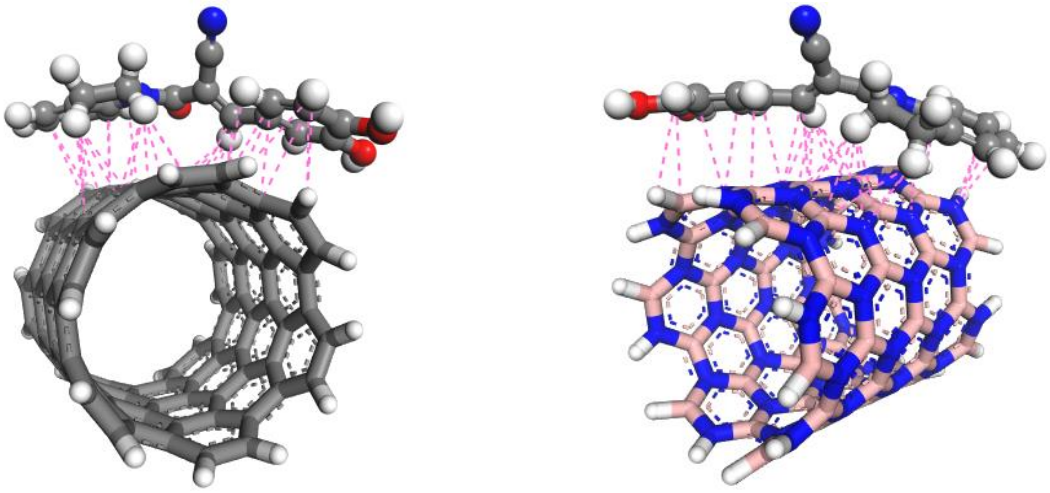

Tyrphostin /SWCNT **Tyrphostin /BNNT**

Figure 1. The most stable adsorption configuration of Tyrphostin/carrier complexes in the adsorption locator module with a close contact of 3 – 3.5Å

3.2 Binding Energy

The interaction of the Tyrphostin inhibitor and the carrier tube can be evaluated with binding energy. The binding energy ($E_{binding}$) is calculated according to equation (1).

$$E_{binding} = E_{\text{Tyrph./}carrier} - \left(E_{carrier} + E_{\text{Tyrph.}}\right) \quad (1)$$

where $E_{\text{Tyrph./carrier}}$ is the total electronic energy of Tyrphostin loaded on a carrier, the $E_{carrier}$ and the $E_{\text{Tyrph.}}$ are, after DMol3 geometry optimization, the individual electronic energies of the pure carrier and Tyrphostin inhibitor, respectively [15]. The Tyrphostin/SWCNT complex binding energy is estimated to be -131.8 kcal/mol. The negative value indicates that the Tyrphostin inhibitor was preferentially adsorbed onto the SWCNT carrier. This value shifts positively to 25702.8 kcal/mol in the case of the Tyrphostin/BBNT complex, thus indicating the presence of an endothermic interaction. However, no chemical bonding was formed during the adsorption process.

3.3. DMol3 Study

3.3.1. Molecular Orbital Analysis

Figure 2 illustrates the lowest unoccupied molecular orbital (LUMO) and the highest occupied molecular orbital (HOMO) of the pure adsorbate, carriers, and their complexes. It is clearly observed that the HOMO orbital of Tyrphostin is localized over a hydrogen atom of the methylene group in the indoline ring, whereas the antibonding character of carbonyl and cyanide groups is involved in the formation of the LUMO

region. This suggests the presence of $\sigma \rightarrow \pi^*$ transition. The HOMO and LUMO orbitals of the SWCNT carrier are localized on the carbon double bonds (-C=C-) of a nanotube implying $\pi \rightarrow \pi^*$. In the case of the BNNT carrier, the HOMO orbitals are distributed over the electron-rich nitrogen atoms, whereas the LUMO orbital appeared over the boron atoms. When Tyrphostin was adsorbed on the SWCNT nanotube, the frontier orbitals of the complex are found to be similar to that of a pure carrier. This evidently indicates that the interaction between Tyrphostin and SWCNT is weak and no chemical bonds occur. The SWCNT can physically act as a proper carrier for the delivery of Tyrphostin. In the case of the Tyrphostin/BNNT complex, there is no charge distribution on the carrier. The HOMO and LUMO orbitals were completely positioned on Tyrphostin. While the HOMO orbital is localized on the carbonyl group, double bonds, and nitrogen atom of the indoline ring, the LUMO orbitals are dispersed in cyanide groups and the phenyl ring's double bonds. In spite of this difference, both drug delivery systems show two types of weak interactions including $-CH-\pi$ and $\pi-\pi$ stackings, as shown in Figure 1. This behavior is in line with other theoretical results [12]. The interaction behavior upon adsorption is usually described by molecular band edge positions of the inhibitor/carrier complex. The molecular band edge positions, band gap energies (E_{gap}), and the corresponding chemical potentials that have been calculated by equations (2 – 3), respectively, are tabulated in Table 2 [16].

$$E_{gap} = (E_{LUMO} - E_{HOMO}) \quad (2)$$

$$\mu = -\left(\frac{E_{HOMO} + E_{LUMO}}{2}\right) \quad (3)$$

A low value of energy gap indicates that the Tyrphostin, SWCNT, and their complex are more reactive; they add electrons to the LUMO orbital, thus being more polarizable and chemically softer. However, the negative values of HOMO and LUMO orbitals reflect neither adding nor removing an electron that may occur [14]. A large energy gap of 4.8 eV for BNNT suggests the presence of an insulating property of the carrier [17]. However, this gap is reduced to 2.35 eV after the interaction with Tyrphostin. These results elucidate that the electronic properties of the BNNT carrier became more sensitive to detect the inhibitor and the complex was converted to soft species.

3.3.2. Density of States (DOS)

The state density analysis of the adsorption complexes, the isolated carriers, and the Tyrphostin inhibitor is shown in Figure 3. As we noted from Figure 3, the BNNT carrier shows a separation between HOMO and LUMO orbitals, indicating its semiconductor nature. The molecular gap value of Tyrphostin almost equals zero in Table 2 suggesting that the inhibitor has a metallic character. The DOS shape of the Tyrphostin/SWCNT is very similar to that of the pure SWCNT carrier. However, the relative intensity of the peaks passes to a high value. This means that more states are available for occupation. In contrast, there is a shift in the peak positions in the case of the Tyrphostin/BNNT complex. The interaction between Tyrphostin and BNNT surfaces was able to lower the LUMO energy value, thus leading to the reduction of the energy gap. This reduction is ascribed to the ability of the Tyrphostin inhibitor to introduce additional molecular energy orbitals in the energy gap region of the BNNT carrier. Though the electronic properties of the tube were changed, this result indicates that the Tyrphostin inhibitor was successfully attached to the nanocarrier surfaces.

HOMO **LUMO**

Tyrphostin

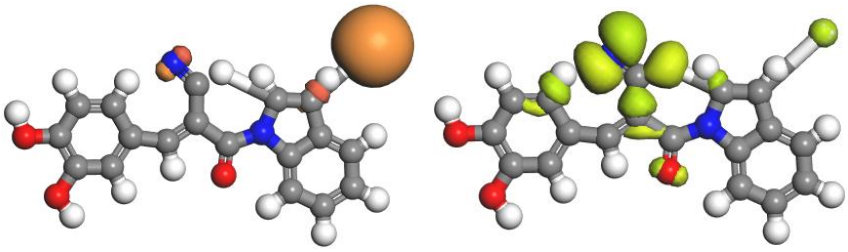

SWCNT

BNNT

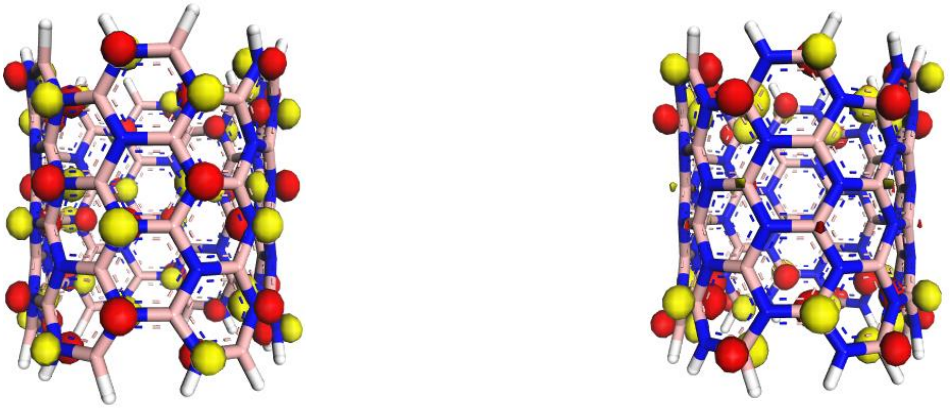

Tyrphostin /SWCNT

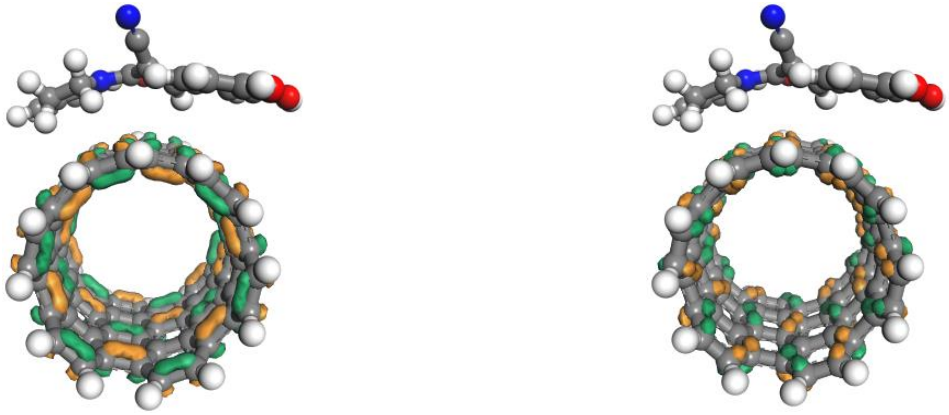

Tyrphostin /BNNT

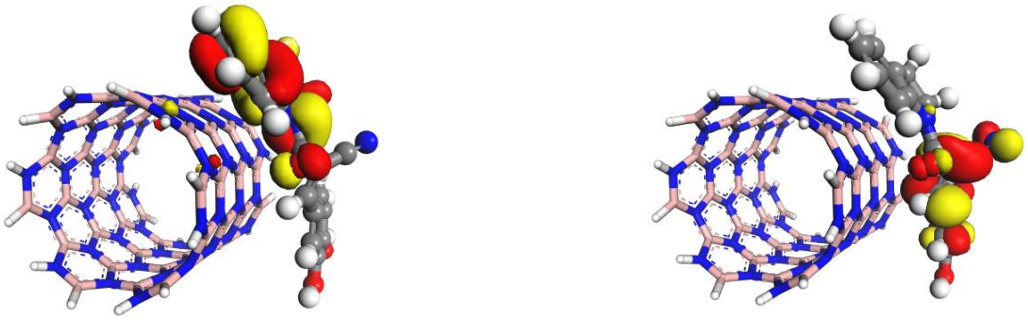

Figure 2. The HOMO and LUMO isosurfaces of the Tyrphostin drug, SWCNT and BNNT carriers, and their complexes

Table 2. The molecular band edge positions, band gap energies and chemical potentials of the studied systems

Parameter (eV)	Tyrphostin	SWCNT	Tyrphostin /SWCNT	BNNT	Tyrphostin /BNNT
E_{HOMO}	-4.642	-3.517	-3.871	-5.433	-5.286
E_{LUMO}	-4.579	-2.789	-3.139	-0.634	-2.933
E_{gap}	0.063	0.728	0.732	4.799	2.353
μ	4.61	3.15	3.51	3.03	4.11

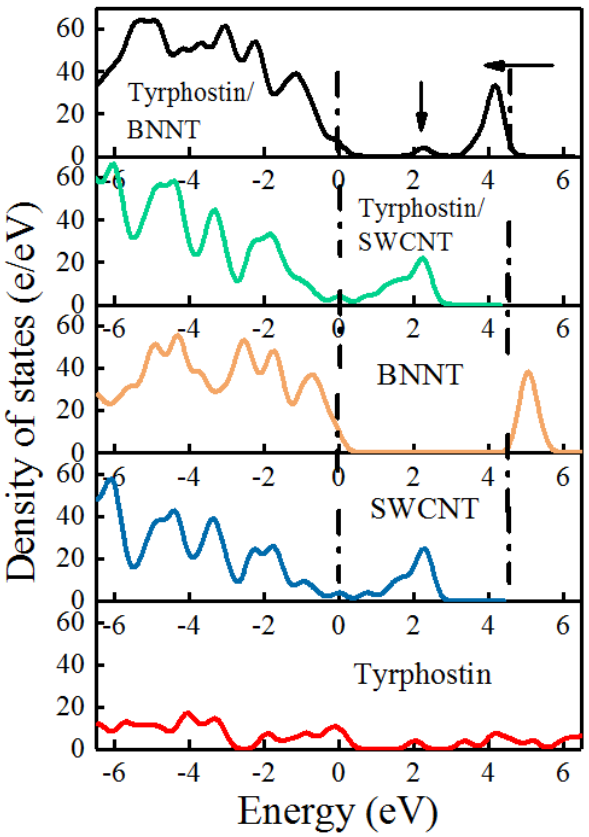

Figure 3. The density of states for the Tyrphostin, SWCNT and BNNT carriers, and their complexes

3.3.3. Optical Properties

The calculations time-dependent-density functional theory (TD-DFT) implemented in the DMol3 module at the GGA/HCTH level of theory were used to investigate whether the interaction of the drug delivery systems produces a significant difference in the optical properties. The simulated spectra of the studied systems are given in Figure 4. Four peaks at 407 nm, 450 nm, 564 nm, and 717 nm are observed on the calculated UV – vis spectrum of the Tyrphostin cancer inhibitor. These electronic transitions with the associated oscillator strengths are given in Table 3. The calculated UV – vis spectra of the Tyrphostin/SWCNT complex and the SWCNT carrier are almost the same. The complex spectrum shows two strong absorption peaks at 707 nm and 588 nm implying that the charge transfer completely occurs toward the carrier. Obviously, the spectrum lies within the visible light wavelengths. This makes the Tyrphostin/SWCNT drug delivery system a good visible-light responsive material, that enables a controlled drug release in cancer therapy. In terms of the Tyrphostin/BNNT complex, there are significant red shifts by 19 nm and 59 nm on the Tyrphostin peak positions of 407 nm and 450 nm, respectively. As Figure 5 shows, the absorption peak at 426 nm is ascribed to the energy excitation from HOMO –1 to the LUMO, whereas the peak at 509 nm is dominated by the HOMO-to-LUMO transition of Tyrphostin. Obviously, the adsorption process results in the longest wavelength band transition of the inhibitor. The last absorption peak of the Tyrphostin/BNNT complex at 359 nm is apparently different from the dominated energy transition that has been produced by the isolated BNNT carrier. As we can understand from Figure 5, this bathochromic behavior is referred to the shift of the excited state center towards the Tyrphostin inhibitor.

Table 3. Absorption band maxima and their molecular orbital contributions of Tyrphostin, SWCNT and BNNT carriers, and their complexes.

Excitation energy (nm)	Oscillator strength	Major contributions
Tyrphostin		
407	0.69	H – 2 → L+1
450	0.45	H – 3 → L+1
564	0.36	H – 1 → L+1
717	0.33	H – 5 →L
SWCNT		

588	0.84	H – 3 → L
707	0. 79	H – 1 → L
Tyrphostin/SWCNT		
591	0.84	H – 3 → L
710	0.79	H – 1 → L
BNNT		
244	0.48	H → L+6
Tyrphostin/BNNT		
359	0.12	H – 9 → L
426	0.59	H – 1 → L
509	0.36	H → L

H and L indicate to the HOMO and LUMO orbitals, respectively

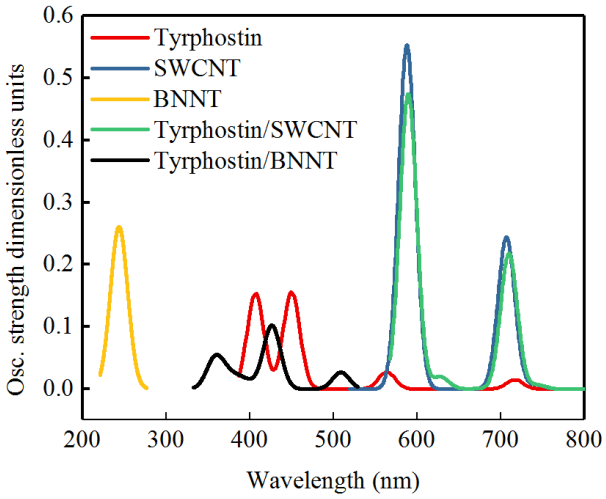

Figure 4. Optical spectra of Tyrphostin, SWCNT and BNNT carriers, and their complexes

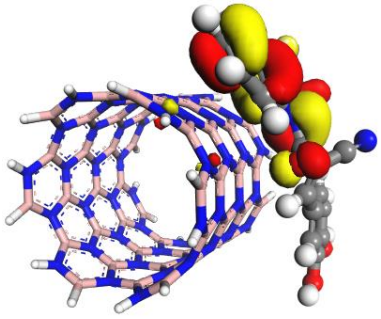

509 nm

HOMO

426 nm

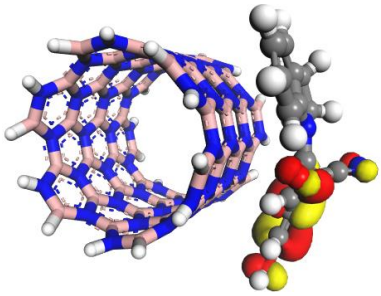

HOMO – 1

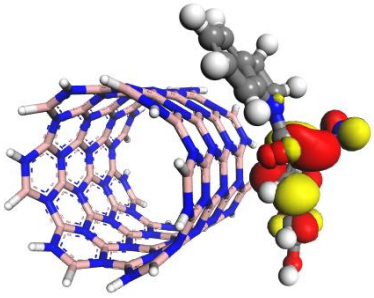

LUMO

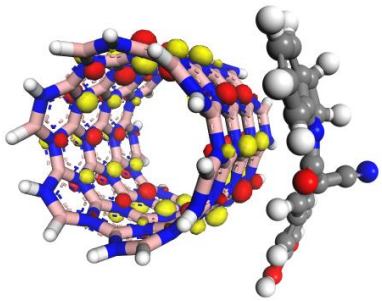

HOMO – 9

Figure 5. Absorption band maxima and their molecular orbital contributions of the Tyrphostin/BNNT complex

3.3.4. COSMO study

The COSMO approach is widely used to describe the affinity of the compounds to interact with each other or with a solvent using a sigma profile (σ −profile). Based on the COSMO theory, there are three regions in the σ −profile curve. The first region is hydrophobic, which is usually taken in a range of -0.01 to 0.01 e/Å^2. Any molecule possessing symmetrical peaks in this region interacts via van der Waals forces. However, any molecule that has a σ −profile value less than -0.01 e/Å^2 can work as a hydrogen bonding donor (HBD). If the σ −profile value is more than 0.01 e/Å^2, the molecule acts as a hydrogen bond acceptor (HBA) [18]. Figures 6 and 7 show the COSMO σ −profile curve and the 3D isosurface of the Tyrphostin inhibitor, pure carriers, and their complexes, which are implemented in the DMol3 module. The extent of the screening charge varies from – 0.015 e/Å^2 (blue) to 0.015 e/Å^2 (red).

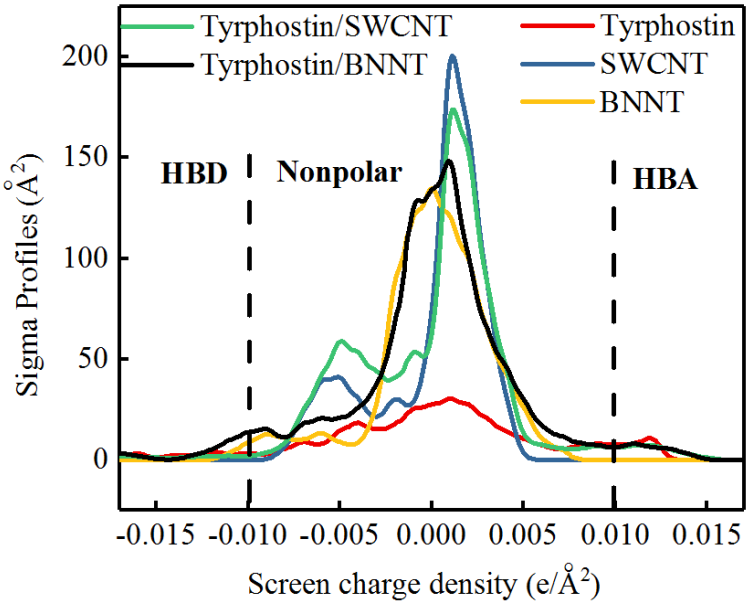

Figure 6. The COSMO sigma profile curves of the Tyrphostin inhibitor, SWCNT and BNNT carriers and their complexes

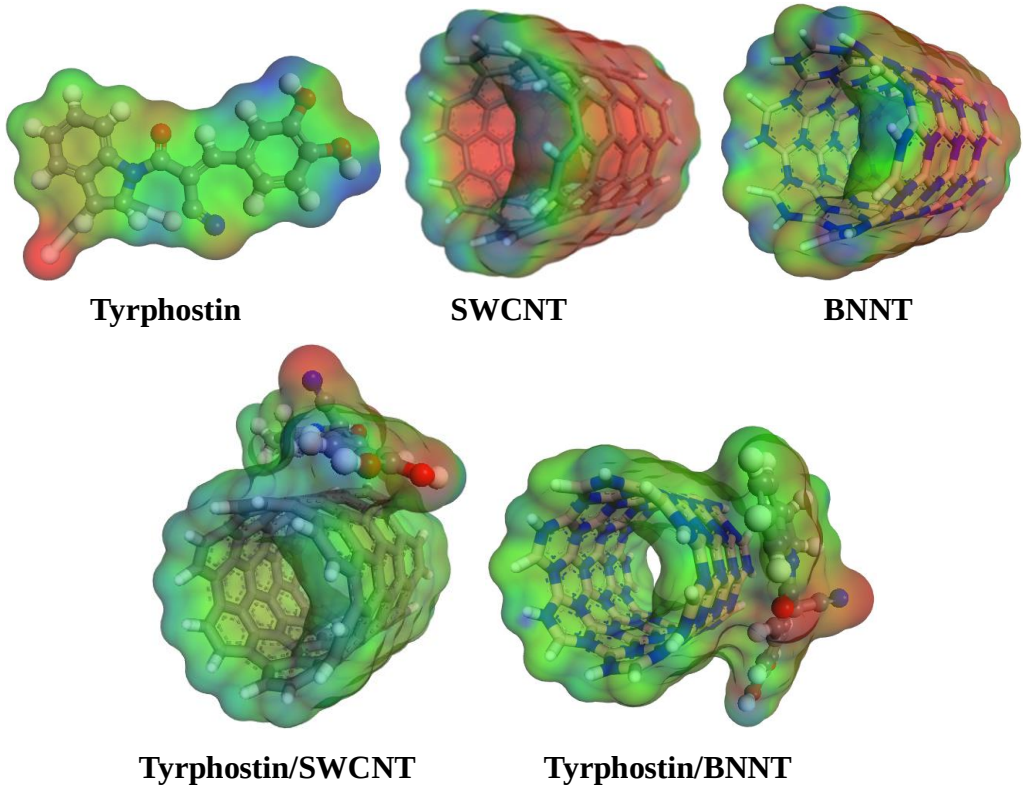

Figure 7. The COSMO 3D surface for the Tyrphostin, SWCNT and BNNT carriers, and their complexes

As shown in Figure 6, all studied systems have peaks distributed significantly in the range of -0.01 to 0.01 e/Å2. This indicates that the systems have a strong repulsive behavior in a hydrophobic

region. The nanotubes can work as effective promising drug delivery carriers for insoluble anticancer drugs. Tyrphostin, however; has a small peak in the HBA region. In comparison, BNNT has a small peak near the HBD region. Obviously, we understand that they have a very small affinity to act as hydrogen bond acceptors and hydrogen bond donors, respectively. The Tyrphostin peaks can be attributed to oxygen atoms, which belong to carbonyl and hydroxyl groups, while the BNNT's peak can easily be referred to nitrogen atoms. It is interesting to note that, in the 3D isosurface, the center of the HOMO orbital can act as a strong electron donor. The $\sigma-$profile curves of the adsorption complexes are similar to that of pure components. However, the 3D surfaces illustrate the presence of a stronger hydrophobic behavior. The HBA affinity shifts towards the nitrogen atom in the cyanide group and towards the oxygen atom in the hydroxyl groups.

3.3.5. The Electrostatic Potential Surface Maps

The non-covalent interaction is usually measured using the electrostatic potential surface (EPS) map, which is also called a molecular electrostatic potential (MEP) map when a positive test charge interacts with a molecule [16]. Figure 8 displays the MEP maps of the Tyrphostin inhibitor, carrier nanotubes, and their adsorption complexes ranging from red to blue. While the red color represents the negative charge, which can work as the preferred site for electrophilic reactions, the blue color indicates the presence of positive charge centers, which are used for nucleophilic reactions. The yellow and green regions are mostly used as an indicator of the neutral electrostatic potential in which the electronegativity difference is not very great [16]. As shown in Figure 8, the positive and negative charges are evenly distributed on the nanotube indicating a nonpolar character of the surface. The centers of the negative charge are mainly distributed inside and outside the SWCNT tube in the area of the delocalized electron bonds. In the BNNT carrier, the negative charge centers are distributed in the vicinity of nitrogen atoms. Considering Tyrphostin, these centers are concentrated on the high electronegative atoms of Oxygen and nitrogen, and in the delocalized electron bonds of the indoline ring. The positive charge centers, however, are localized at the edges of the nanotube due to the presence of hydrogen atoms and in the vicinity of boron atoms along the tube.

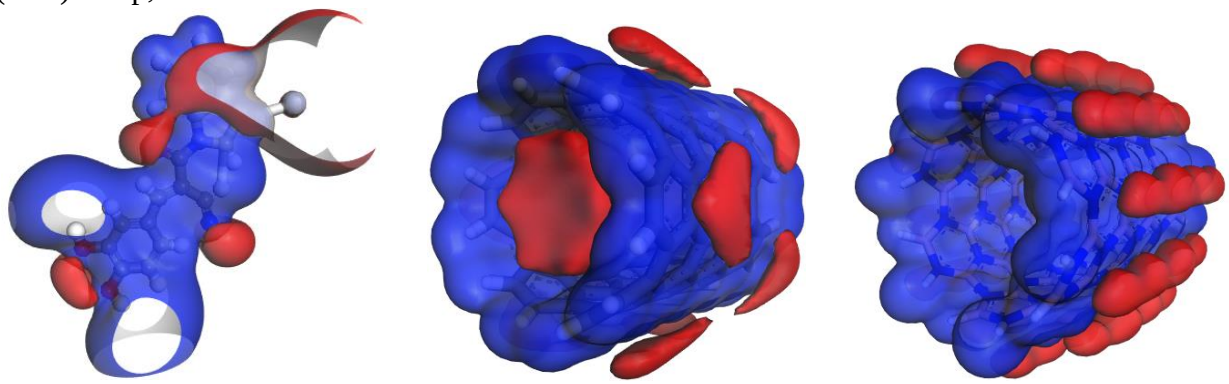

Tyrphostin **SWCNT** **BNNT**

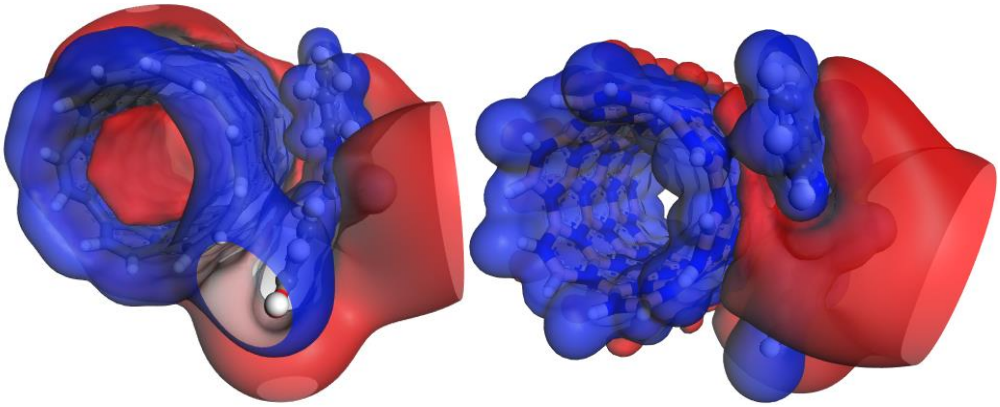

Tyrphostin/SWCNT **Tyrphostin/BBNT**

Figure 8. Molecular electrostatic potential maps of Tyrphostin, SWCNT and BNNT carriers, and their complexes

After adsorption, Figure 1 illustrates that the Tyrphostin hydrogen atoms have a close contact of 3 – 3.5Å. However, high electronegative atoms are pointed away from the nanocarrier surface. In other words, Tyrphostin is attached to the nanotube surface by electrostatic attraction occurring between its positive charge centers and the negative charge centers of the nanotubes. Fan *et al.* (2017); however, ascribed this behavior to the presence of weak kinds of interactions, which are called $-CH-\pi$ and $\pi-\pi$ stackings [12].

4. Conclusion

In the present study, the electronic and optical properties of the Tyrphostin inhibitor on the surface of the SWCNT and BNNT nanocarriers have been investigated by using the DFT and Monte Carlo simulation. The frontier orbital energies, density of states, optical spectra, and molecular electrostatic potential diagrams have been analyzed in details for a better understanding of the interaction mechanism. Theoretical calculations have revealed that the interaction between Tyrphostin and the nanocarriers is an exothermic process. The electrostatic attraction can be attributed to the presence of two kinds of weak van der Waals forces, namely; $-CH-\pi$ and $\pi-\pi$ stackings. The Tyrphostin/SWCNT complex can reproduce the electronic properties of the SWCNT nanocarrier. However, a great change in the electronic properties of the Tyrphostin/BNNT complex is due to the ability of Tyrphostin to reduce the gap within the energy window of the BNNT carrier. There is a significant bathochromic shift in the optical response towards visible light. This makes the Tyrphostin/SWCNT complex a better visible-light response drug delivery system. Both complexes show a strong repulsive towards the water solvent, so they can be used as promising hydrophobic drug delivery systems.

In short, this study attempts underline single-walled carbon and boron nitride nanotubes as important potential candidates for delivery of the Tyrphostin cancer inhibitor. However, what is the prospective role of these nanocarriers when Tyrphostin is targeting the signaling proteins needs to be addressed.

Acknowledgments

This research has no acknowledgments.

Disclosure statement

Conflict of interests: The authors declare that they

have no conflict of interest.
Ethical approval: All ethical guidelines have been adhered.
Sample availability: Samples of the compounds are available from the author.

Funding

This research received no external funding.

ORCID
Eshraq Ahmed Abdullah
https://orcid.org/0000-0001-9698-6203

References

[1] Z. Peng, A. Pal, D. Han, S. Wang, D. Maxwell, A. Levitzki, M. Talpaz, N. J. Donato, and W. Bornmann, "Tyrphostin-like compounds with ubiquitin modulatory activity as possible therapeutic agents for multiple myeloma," *Bioorganic & medicinal chemistry*, vol. 19, no. 23, pp. 7194-7204, 2011.

[2] M. Khattab, S. Chatterjee, A. H. Clayton, and F. Wang, "Two conformers of a tyrosine kinase inhibitor (AG-1478) disclosed using simulated UV-Vis absorption spectroscopy," *New Journal of Chemistry*, vol. 40, no. 10, pp. 8296-8304, 2016.

[3] C.-H. Li, C.-Y. Fang, M.-H. Chan, C.-L. Chen, P.-J. Lu, L.-P. Ger, Y.-C. Chang, and M. Hsiao, "The activation of EP300 by F11R leads to EMT and acts as a prognostic factor in triple-negative breast cancers," vol. **PREPRINT** (Version 1) available at Research Square [https://doi.org/10.21203/rs.3.rs-1454643/v1], 2022.

[4] Q. Jiao, L. Bi, Y. Ren, S. Song, Q. Wang, and Y.-s. Wang, "Advances in studies of tyrosine kinase inhibitors and their acquired resistance," *Molecular cancer*, vol. 17, no. 1, pp. 1-12, 2018.

[5] O. C. Adekoya, G. J. Adekoya, E. R. Sadiku, Y. Hamam, and S. S. Ray, "Application of DFT calculations in designing polymer-based drug delivery systems: an overview," *Pharmaceutics*, vol. 14, no. 9, pp. 1972, 2022.

[6] H. Shaki, H. Raissi, F. Mollania, and H. Hashemzadeh, "Modeling the interaction between anti-cancer drug penicillamine and pristine and functionalized carbon nanotubes for medical applications: Density functional theory investigation and a molecular dynamics simulation," *Journal of Biomolecular Structure and Dynamics*, vol. 38, no. 5, pp. 1322-1334, 2020.

[7] P. Trucillo, "Drug carriers: Classification, administration, release profiles, and industrial approach," *Processes*, vol. 9, no. 3, pp. 470, 2021.

[8] M. Sheikhi, S. Shahab, R. Alnajjar, M. Ahmadianarog, and S. Kaviani, "Investigation of adsorption tyrphostin AG528 anticancer drug upon the CNT (6, 6-6) nanotube: a DFT study," *Current Molecular Medicine*, vol. 19, no. 2, pp. 91-104, 2019.

[9] M. Z. Dehaghani, B. Bagheri, F. Yousefi, A. Nasiriasayesh, A. H. Mashhadzadeh, P. Zarrintaj, N. Rabiee, M. Bagherzadeh, V. Fierro, and A. Celzard, "Boron nitride nanotube as an antimicrobial peptide carrier: a theoretical insight," *International Journal of Nanomedicine*, vol. 16, pp. 1837—1847, 2021.

[10] S. Kalay, Z. Yilmaz, O. Sen, M. Emanet, E. Kazanc, and M. Çulha, "Synthesis of boron nitride nanotubes and their applications," *Beilstein journal of nanotechnology*, vol. 6, no. 1, pp. 84-102, 2015.

[11] A. Mortazavifar, H. Raissi, and M. Shahabi, "Comparative prediction of binding affinity of Hydroxyurea anti-cancer to boron nitride and carbon nanotubes as smart targeted drug delivery vehicles," *Journal of Biomolecular Structure and Dynamics*, vol. 37, no. 18, pp. 4852-4862, 2019.

[12] G. Fan, S. Zhu, K. Ni, and H. Xu, "Theoretical study of the adsorption of aromatic amino acids on a single-wall boron nitride nanotube with empirical dispersion correction," *Canadian Journal of Chemistry*, vol. 95, no. 6, pp. 710-716, 2017.

[13] C. H. Lee, S. Bhandari, B. Tiwari, N. Yapici, D. Zhang, and Y. K. Yap, "Boron nitride nanotubes: recent advances in their synthesis, functionalization, and applications," *Molecules*, vol. 21, no. 7, pp. 922, 2016.

[14] E. A. Abdullah, "Theoretical study of a single-walled carbon nanotube and a cellulose biofiber as 5-fluorouracil anti-cancer drug carriers," *European Journal of Chemistry*, vol. 13, no. 1, pp. 69-77, 2022.

[15] S. Bibi, S. Ur-Rehman, L. Khalid, I. A. Bhatti, H. N. Bhatti, J. Iqbal, F. Q. Bai, and H.-X. Zhang, "Investigation of the adsorption properties of gemcitabine anticancer drug with metal-doped boron nitride fullerenes as a drug-delivery carrier: a DFT study," *RSC advances*, vol. 12, no. 5, pp. 2873-2887, 2022.

[16] E. A. Abdullah, "Electronic band structure of Bi5O7NO3 and its methyl orange removal mechanism," *European Journal of Chemistry*, vol. 13, no. 3, pp. 337-350, 2022.

[17] N. Saikia, A. N. Jha, and R. C. Deka, "Interaction of pyrazinamide drug functionalized carbon and boron nitride nanotubes with pncA protein: a molecular dynamics and density functional approach," *RSC Advances*, vol. 3, no. 35, pp. 15102-15107, 2013.

[18] M. A. Mohammad Alwi, E. Normaya, H. Ismail, A. Iqbal, B. Mat Piah, M. A. Abu Samah, and M. N. Ahmad, "Two-Dimensional infrared correlation spectroscopy, conductor-like screening model for real solvents, and density functional theory study on the adsorption mechanism of polyvinylpolypyrrolidone for effective phenol removal in an aqueous medium," *ACS omega*, vol. 6, no. 39, pp. 25179-25192, 2021.